

## BIROn - Birkbeck Institutional Research Online

Odlyha, Marianne and Lucejko, J.J. and Lluveras-Tenorio, A. and di Girolamo, F. and Hudziak, S. and Strange, A. and Bridarolli, A. and Bozec, L. and Colombini, M.P. (2022) Violin varnishes: microstructure and nanomechanical analysis. *Molecules* 27 (19), p. 6378. ISSN 1420-3049.

Downloaded from: <https://eprints.bbk.ac.uk/id/eprint/50045/>

*Usage Guidelines:*



Please refer to usage guidelines at <https://eprints.bbk.ac.uk/policies.html>

or alternatively

contact [lib-eprints@bbk.ac.uk](mailto:lib-eprints@bbk.ac.uk).

Article

# Violin Varnishes: Microstructure and Nanomechanical Analysis

Marianne Odlyha <sup>1,\*</sup>, Jeannette J. Lucejko <sup>2</sup>, Anna Lluveras-Tenorio <sup>2</sup>, Francesca di Girolamo <sup>2</sup>, Stephen Hudziak <sup>3</sup>, Adam Strange <sup>4</sup>, Alexandra Bridarolli <sup>4,5</sup>, Laurent Bozec <sup>4,5,6</sup> and Maria Perla Colombini <sup>2,\*</sup>

<sup>1</sup> Department of Biological Sciences, Birkbeck, University of London, London WC1E 7HX, UK

<sup>2</sup> Department of Chemistry and Industrial Chemistry, University of Pisa, Via Giuseppe Moruzzi 13, 56127 Pisa, Italy

<sup>3</sup> Department of Electronic and Electrical Engineering, University College London, London WC1E 6BT, UK

<sup>4</sup> Eastman Dental Institute, University College London, London WC1E 6DG, UK

<sup>5</sup> Getty Conservation Institute, 1200 Getty Center Drive, Suite 700, Los Angeles, CA 90049, USA

<sup>6</sup> Faculty of Dentistry, University of Toronto, Toronto, ON M5G 1G6, Canada

\* Correspondence: m.odlyha@bbk.ac.uk (M.O.); maria.perla.colombini@unipi.it (M.P.C.)

**Abstract:** The aim of the current work is twofold: to demonstrate the application of in situ non-invasive imaging by portable atomic force microscopy (AFM) on the surfaces of a violin and to integrate compositional and mechanical analysis at the nano scale level on model samples of varnished wood. These samples were prepared according to traditional recipes by an Italian lute-maker family well practised in the art. Samples of oil and spirit-based varnishes on maple wood, naturally and accelerated light aged, were studied. AFM was used to measure the nanomechanical properties of the model samples and established that the spirit-based varnish was stiffer than the oil-based. Synchrotron radiation micro- Fourier Transform Infra-red analysis of the layer structure revealed that stiffer spirit-based varnish showed less penetration into the wood than the oil-based. Further PeakForce Quantitative Nanomechanical Mapping (QNM) demonstrated a difference in adhesion values between the oil- and spirit-based samples.

**Keywords:** in situ imaging; AFM; SR micro-FTIR; violin; nanomechanics



**Citation:** Odlyha, M.; Lucejko, J.J.; Lluveras-Tenorio, A.; di Girolamo, F.; Hudziak, S.; Strange, A.; Bridarolli, A.; Bozec, L.; Colombini, M.P. Violin Varnishes: Microstructure and Nanomechanical Analysis. *Molecules* **2022**, *27*, 6378. <https://doi.org/10.3390/molecules27196378>

Academic Editor: Giuseppe Cirillo

Received: 31 August 2022

Accepted: 22 September 2022

Published: 27 September 2022

**Publisher's Note:** MDPI stays neutral with regard to jurisdictional claims in published maps and institutional affiliations.



**Copyright:** © 2022 by the authors. Licensee MDPI, Basel, Switzerland. This article is an open access article distributed under the terms and conditions of the Creative Commons Attribution (CC BY) license (<https://creativecommons.org/licenses/by/4.0/>).

## 1. Introduction

To date, in the conservation of musical instruments, it has been a challenge to understand the effect of the varnishing process on wood and whether this process affects the overall performance of varnished wooden instruments. A recent paper by Gilani showed that laboratory varnishes with various compositions penetrated differently into the wood structure [1] as recorded by non-destructive methods such as vibration tests and X-ray tomography. A comprehensive review has also been made of the chemical composition and multi-layered structure of varnishes of historical musical instruments, in particular stringed instruments of the violin family from the 17th and 18th centuries [2]. In the current paper, the information on depth penetration of varnishes of different chemical composition is combined with their mechanical properties measured at the nano-scale. This follows on from previous studies where attention was directed to the physicochemical state of varnish and how this affects the mechanical response of wood [3–5]. It was observed that the stiffness of the wood measured in tension in the radial direction increased in the presence of the dammar varnish layer and these results were consistent with what was reported previously using a theoretical approach on spruce plates with natural resins [6]. There was also difference in the mechanical properties and response to relative humidity (RH) of varnished wood panels (pine) stored within protected enclosures such as micro-climate frames and showcases and outside these enclosures together with a difference in the surface topography of the varnished surfaces. It has recently been shown that even preparatory treatments affect the properties of the wood and certainly influence subsequent penetration of the varnish [7].

Several papers reported analytical study on varnishes [4,8–10]. For example studies on historical stringed musical instruments from the collection of the Vincenzo Bellini Conservatory in Palermo (Italy) showed that the varnish on all the sampled instruments has a consistent formulation containing a mixture of a diterpenoid resin, shellac and a drying oil [11]. Chemical analysis at the molecular level using gas chromatography and mass spectrometry (GC/MS) showed differences in the chemical composition of varnished panels maintained within and outside the enclosures [12]. Recently, the composition of the materials and the chemical composition of each varnish layer was reported by using spatially resolved synchrotron radiation micro-FTIR spectroscopy (SR-FTIR), which included studies on early 18th century musical instruments [13], a late 16th cent. Venetian lute [14] and instruments which were undisputed representative examples of Stradivari's work [15].

An important consideration in the evaluation of the state of preservation of a string instrument is the application of non-invasive and non-destructive techniques. For this reason, optical coherence tomography (OCT) [16] has been applied. A recent *in situ* study of the surface of an 18th century Italian violin provided important information for its conservation treatment and demonstrated that it was possible to characterize the thickness of varnish layers and image the three-dimensional wood structures below the varnishes [17]. The relevance of the mechanical properties of varnishes has recently been highlighted [3]. To achieve a non-invasive non-destructive approach, the use of force spectroscopy with Atomic Force Microscopy (AFM) could be considered, and, in this paper, a preliminary study on model samples is included (Table 1, described in Section 4.1.2). Force spectroscopy with AFM has emerged as a powerful technique as it is able to provide information on the nanomechanical properties of a wide variety of materials at the nanometre/nanonewton scale [18]. At this stage, *in situ* AFM imaging has been achieved on 18th cent parchment. It was possible to detect changes in the collagen in parchment, which can cause surface cracking resulting in loss of text and can increase the vulnerability of parchment to aqueous cleaning agents [19]. In the literature, there are few studies using AFM to evaluate the surface properties of woods. An early report by Vlad-Cristea et al. [20] used both nanoindentation and atomic force microscopy to investigate whether the exterior durability of waterborne coatings improved with inorganic nanosized UV-absorbers. In their study, AFM was used to detect the very early stages of surface roughening and blistering that occurs during weathering. The recent research by Mao et al. [21] presents an accurate atomic force microscopy (AFM) method of investigating wood aging. The team's work demonstrated a novel AFM-based method of analysing wood aging. The technique was able to characterize changes to the wood surface by measuring the relative adhesion force between the wood sample and the AFM tips. It was concluded that the structures most suitable for monitoring aging at early stages were the wood pits. Others have used AFM to characterize the entire wood cell wall mechanically at the nanometre level [22,23]. Recently, Czibula et al. [24] demonstrated a decreasing trend in the longitudinal and transverse viscoelastic properties of wood pulp fibers at different relative humidity. However, they hypothesised that the unknown microfibril angle (MFA) and the anisotropy of the material could have an influence on the results.

The current work is aimed at evaluating the feasibility of *in situ* imaging by using Atomic Force Microscopy (AFM) not only on reference systems simulating the stratigraphy of a violin but also on a historical violin in order to obtain information on the preservation of the varnished surface. *In situ* AFM does not require sampling as the instrument is fully portable and would allow for *in situ* examination of the varnish surface at the nanoscale level. To complement surface information, chemical analysis using micro-Fourier Transform Infra-red analysis has also been performed. Actually, Infra-red specular reflection and diffuse-transflection techniques have been reported as a method for *in situ* non-destructive analyses of varnishes on historical violins with a view to indicate state of degradation of varnishes [25,26]. A recent paper on modified asphalt binders [27] and on bamboo fibre cell walls and their composites has demonstrated the value of these additional data as basic

nanomechanistic properties, adhesion, energy dissipation, and deformation of the modified asphalt binders were determined [28].

This paper reports the results obtained by in situ AFM imaging on a historical violin bought in 1946 from Boosey & Co in London and Synchrotron radiation micro-FTIR spectroscopy (SR-FTIR) on model system samples (Table 1, described in Section 4.1.2) prepared by a violin maker (Gabriele Carletti who continued the family tradition of constructing and restoring string instruments) according to traditional recipes. In addition, force spectroscopy with AFM and peakForce QNM mode of AFM were used to measure the nano mechanical properties of model violin samples and to provide information on adhesion values of the surfaces.

## 2. Results and Discussion

Atomic force microscopy (AFM) was applied to violin surface analysis. The AFM head was placed directly on the instrument as shown in Figure 1a, and the whole violin was placed on an anti-vibration table. Figure 1b shows the tip in contact with the surface. To the right side in Figure 1b it is possible to see one of the legs resting on a plastic spacer used to protect the surface of the violin on which the AFM head rested. It was found that operation in intermittent contact mode provided better images. Figure 1c,d show the resulting AFM images taken in different locations on the surface of the violin. The surface shows the directional nature of varnish application following the direction of the grain of the wood, some small deformations, and some particulate matter. This is the first time that it has been demonstrated that it is possible to image directly the surface of a violin using AFM. The ability to visualise the surface at the nanoscale level provides information on the state of preservation of the varnish and may indicate the type of preparation used. AFM has been previously used in studies on violins, in particular in the study of structural changes in cuticles on violin bow hair caused by wear and in comparison of synthetic hair and natural horse tail as used in professional orchestras [29,30].

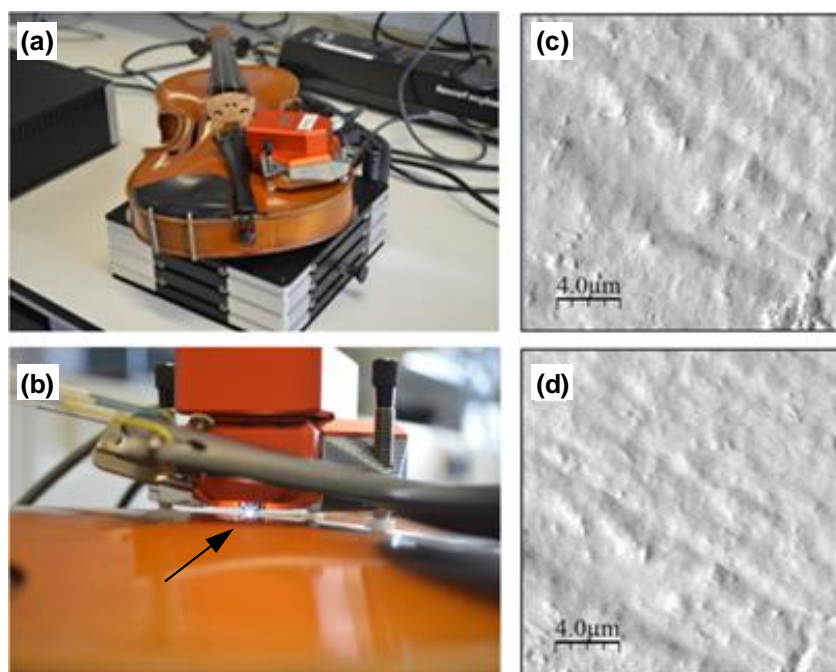


**Figure 1.** (a) Nanosurf Easyscan 2 AFM head on a violin placed on an anti-vibration table (b) closer view of AFM head on the violin placed on plastic spacers to protect the surface of the violin and showing location of the AFM tip (black arrow) (c,d) AFM images ( $20\ \mu\text{m} \times 20\ \mu\text{m}$ ) recorded directly on the violin surface in two different locations [location (c) z-scale image =  $1.28\ \mu\text{m}$ /Roughness Ra  $0.176\ \mu\text{m}$ ; location (d) z-scale image =  $2.03\ \mu\text{m}$ /Roughness Ra  $0.291\ \mu\text{m}$ ].

The second aim of this study was to evaluate the mechanical properties of the varnished surfaces at the nanoscale level. For these measurements, a set of model varnish samples was prepared according to traditional practices for violins. Table 1, described in Section 4.1.2 shows the recipes used in the preparations. AFM has long been recognised as a useful instrument for the evaluation of local mechanical properties of materials. A collection of force–distance curves at each pixel allows for mapping of the elastic properties [31]. Recent advances in Force spectroscopy with AFM have meant that additional material properties such as dissipation, adhesion, and deformation are mapped simultaneously with topography at nanoscale resolution [18,32]. Figure 2 shows corresponding AFM images (10  $\mu\text{m} \times 10 \mu\text{m}$ ) of the model samples. Several locations were tested. Naturally aged samples (4 years) and accelerated aged samples (2 weeks of Solar box) were studied.

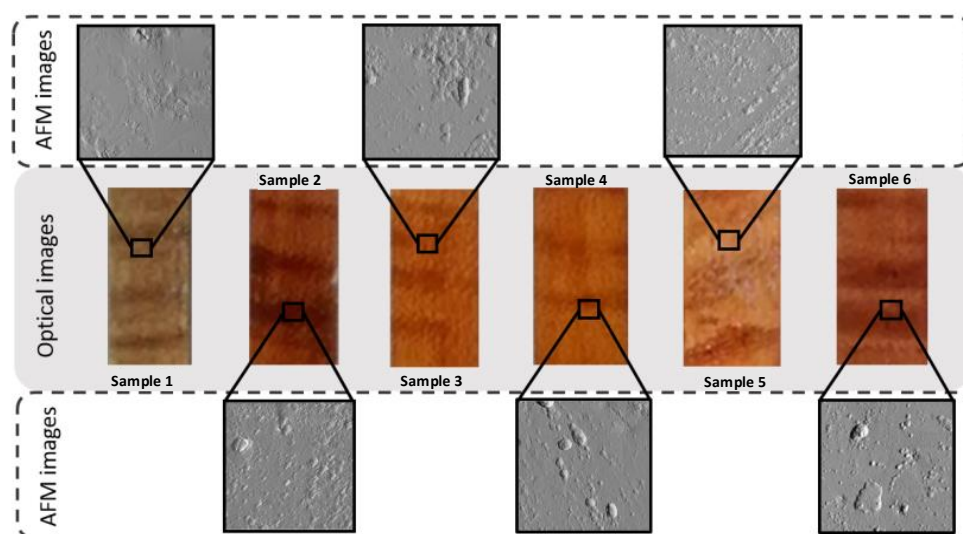


**Figure 2.** Model systems optical images together with AFM images of samples (1 to 6) before ageing: oil-based (1 and 5); AFM image 1, z scale image = 159.4 nm/Roughness 19.1 nm; AFM image 5, z scale image = 164.5 nm/Roughness 18.2 nm; and spirit-based varnish layers (2, 3, 4, 6); AFM image 2 z scale image = 235.6 nm/Roughness 10.5 nm; AFM image 3, z scale image = 522.6 nm/Roughness 33.6 nm; AFM image 4, z scale image = 823.9 nm/Roughness 18.6 nm; AFM image 6, z scale image = 260.0 nm/Roughness 14.5 nm on top of maple wood over preparation layers of various compositions (Table 1, described in Section 4.1.2).

With regard to the mechanical properties of these samples measured at the nanoscale level, Young’s modulus values were calculated from the measured force distance curves obtained from AFM. This information was complemented with chemical analysis of the layers in the varnished wood samples’ cross-sections using synchrotron radiation micro-Fourier Transform Infra-red analysis. Figures 3 and 4 show the spectral and the mechanical data for both naturally aged and accelerated aged oil based varnish sample 1 (Figure 2), and spirit-based varnish sample 6 (Figure 2).

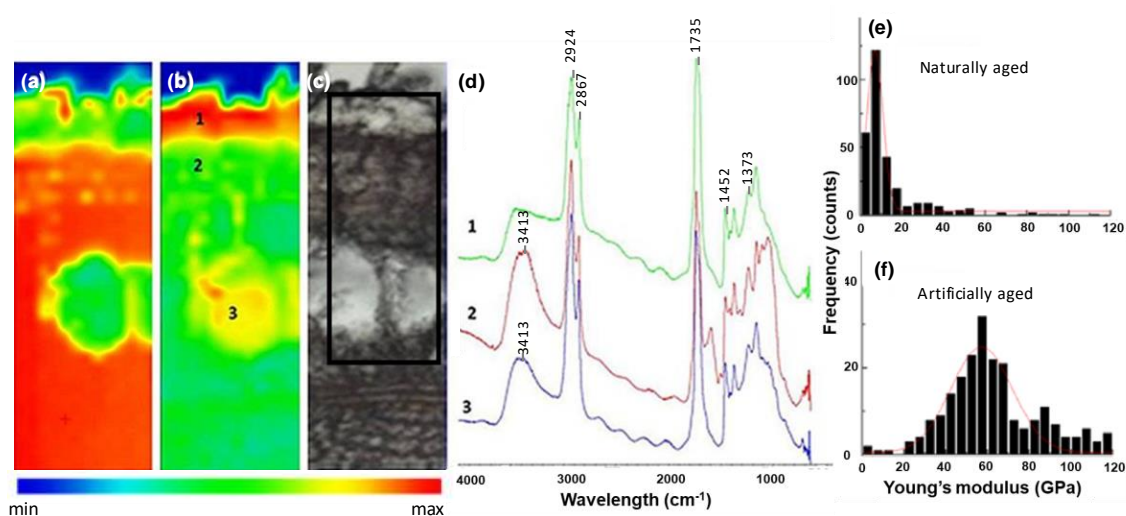


**Figure 3.** (a–d) shows SR-micro-FTIR mapping for the naturally aged oil-based varnish (Figure 2 sample 1): chemical image mapping of the absorbance at (a)  $1000\text{ cm}^{-1}$  and (b)  $1735\text{ cm}^{-1}$ , respectively, and (c) photomicrograph of the microtomed cross-section of width  $10\text{ }\mu\text{m}$ . (the squared area outlined in black has a depth of  $250\text{ }\mu\text{m}$  and indicates depth of penetration of the oil into the wood); and (d) FTIR spectra of layers (1, 2, 3) as shown in (b) and corresponding to varnish, penetration areas of oil in wood, and oil, indicating high penetration into the wood porous structure (around  $200\text{ }\mu\text{m}$ ). (e,f) shows mechanical data and distribution of Young's modulus in the unaged which, at time of analysis, had undergone four years of natural ageing in the dark (e) and the artificially accelerated aged sample (f) where median values of Young's modulus are  $(7.04 \pm 1.75)\text{ GPa}$  and  $(57.2 \pm 5.1)\text{ GPa}$ , respectively.

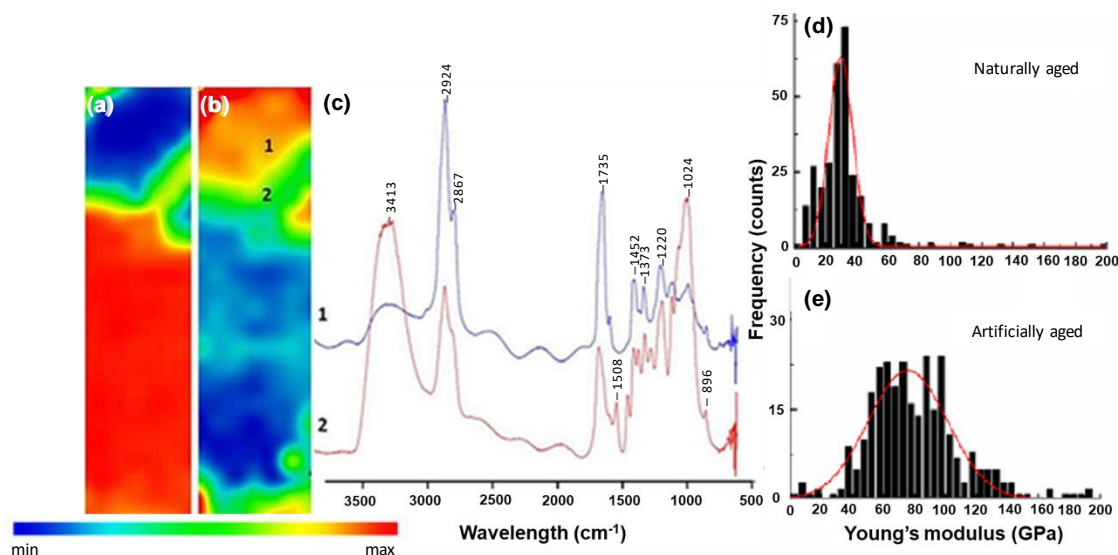


**Figure 4.** (a–c) shows SR-micro-FTIR mapping of the naturally aged spirit-based varnish (Figure 2 sample 6): chemical image mapping the absorbance at  $1000\text{ cm}^{-1}$  (a) and  $1700\text{ cm}^{-1}$  (b) respectively. FTIR spectra (c) representative of the varnish layer (1-blue line) and the underlying wood (2-red line) in (b). The spirit-based varnish remains on the surface with a clear separation from the wood as shown by the difference in spectra for layers 1 and 2. (d,e) shows mechanical data and distribution of Young's modulus in naturally aged (4 years) (d) and artificially accelerated aged (e) samples where median values of Young's modulus are  $29.7 \pm 3.1\text{ GPa}$  and  $75.7 \pm 9.1\text{ GPa}$ , respectively.

Oil-based varnish shows a characteristic C=O stretching vibration centred at  $1735\text{ cm}^{-1}$  with a shoulder at  $1708\text{ cm}^{-1}$ , characteristic of the ester linkages of the triglycerides from the drying oil and the free fatty acids formed during its ageing. FTIR spectra of the varnish

layers of the oil-based sample in Figure 3d showed typical bands for oil-based varnish (i.e., the strong and broad carbonyl stretching absorption and some medium intensity absorption bands at  $1452\text{ cm}^{-1}$ ,  $1373\text{ cm}^{-1}$  (from the resin component also present) and accompanying alkyl stretching bands). Strong peaks with two maxima at  $2924\text{ cm}^{-1}$  and  $2867\text{ cm}^{-1}$  are due to aliphatic C-H stretch of alkyl groups. The numbers (1 to 3) in Figure 3b,d refer to the different composition areas: 1 contains oil varnish, 2 contains wood and oil varnish and 3 contains oil varnish on the layer of wood support, being the result of the penetration of the varnish.

The FTIR data for the spirit-based sample (Figure 4c) show a C=O stretching band centred at  $1696\text{ cm}^{-1}$  and two medium intensity absorption bands at  $1452\text{ cm}^{-1}$ ,  $1373\text{ cm}^{-1}$  which highlight the presence of a terpenoid resin [13]. These spectra also show strong peaks with two maxima at  $2924\text{ cm}^{-1}$  and  $2867\text{ cm}^{-1}$  corresponding to aliphatic C-H stretch of alkyl groups, which are more intense in the varnish layer (blue line) than in the wood (red line). Chemical maps of the spirit based model show that varnish remains on the surface with a clear separation from the wood as shown by the difference in spectra for layers 1 and 2 (Figure 4c).

The FT-IR spectra of the wood layer in both Figures 3 and 4 show a broadening to lower wavenumbers of the band at  $3413\text{ cm}^{-1}$ . This may be caused by the residual water present in the wood layer due to the fact that the wood is a highly hygroscopic material but also due to O-H stretching vibration from alcohols ( $3600\text{--}3300\text{ cm}^{-1}$ ) and carboxylic acids ( $3300\text{--}2500\text{ cm}^{-1}$ ), present either in polysaccharides or lignin fractions of wood [33,34]. The broad band between  $900$  and  $1100\text{ cm}^{-1}$  in Figure 4c (red line) contains many signals from cellulose vibrational modes, in particular, the band at  $1024\text{ cm}^{-1}$  related to the C-O bond. At  $896\text{ cm}^{-1}$  the typical signal for C-H stretching involving C1 carbons in the glucose ring is visible. The absorption band at  $1508\text{ cm}^{-1}$ , attributed to aromatic skeletal vibrations in lignin as well as the band at  $1220\text{ cm}^{-1}$  [33,35,36] is also present.

Figures 3 and 4a,b show the chemical images at  $1000\text{ cm}^{-1}$  and  $1700\text{ cm}^{-1}$  and the distribution of the wood support and the varnish, respectively. From the FTIR maps, it is possible to observe the degrees of penetration of the varnish layers into the wood support. The oil-based varnish shows a high penetration into the wood porous structure (around  $200\text{ }\mu\text{m}$ ) (Figure 3d) while the spirit based one remains on the surface with a clear separation from the wood support (Figure 4c).

Figure 3d,e shows the distribution of Young's modulus of the varnished wood oil-based sample. In the accelerated aged sample, there is a clear shift in the maximum of the distribution of Young's modulus to higher values, i.e.,  $60\text{ GPa}$  (Figure 3f). There is also a broader distribution in the aged sample. The maximum value of Young's modulus for the unaged sample, which had been naturally aged (4 years) at the time of analysis, lies in the range  $5\text{--}10\text{ GPa}$ , and this correlates with values found for maple (hardwood) (elastic modulus  $12.62\text{ GPa}$ ) [37].

Figure 4d,e shows the distribution of Young's modulus on the varnished wood spirit-based sample, sample 6. In the unaged sample (Figure 4d), which had also been naturally aged (4 years) at the time of analysis, the maximum value for the modulus is higher than in the oil-based sample and is in the region  $30\text{--}40\text{ GPa}$ . In the accelerated aged spirit-based sample, there is also a shift in the maximum of the distribution of Young's modulus to higher values but the distribution of the aged sample ( $60\text{--}100\text{ GPa}$ ) is broader (Figure 4e) than in the oil-based sample.

Nanomechanical measurements were also performed on samples 2, 3, 4 and 5 (Figure 5). The spirit-based samples (black bars) show similar values of modulus to that of sample 6. The second oil-based sample (sample 5 grey bars) has a higher modulus value, unlike that of the other oil-based sample (sample 1), and also differs from sample 6 as seen in the adhesion data below.

Information on adhesion values of the surfaces of the model violin samples was also obtained. The PeakForce Adhesion image of the naturally aged spirit-based sample (sample 6, Figure 2) is shown in Figure 6a, and the image for the naturally aged oil-based varnish

(sample 5, Figure 2) is shown in Figure 6b. These were recorded from PeakForce QNM measurements. Bearing analysis showed that the two samples gave large differences in the distribution of adhesion values, Figure 6c. The spirit-based sample has a higher maximum adhesion value than the oil-based sample with a broader distribution of values. The oil-based sample (sample 1, Figure 2) has a lower maximum adhesion value and a narrower range of values. Figure 6b shows that the distribution of adhesion values for the spirit-based varnish can be resolved into two contributions to the overall peak, corresponding to regions of lower and higher adhesion values as seen in the image in Figure 6a. This could be a future marker that can be used to characterise behaviour of spirit-based varnishes. Further work is in progress.

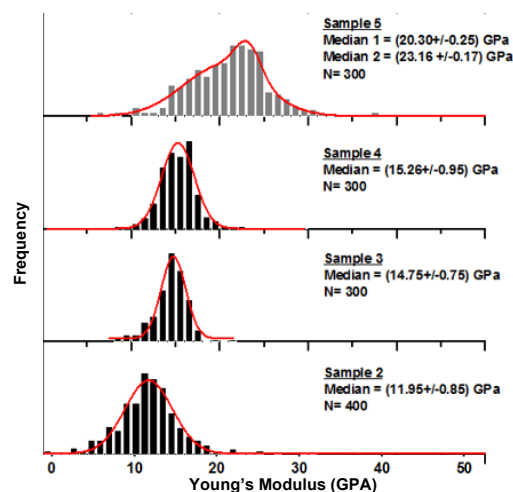


Figure 5. Mechanical data and distribution of Young's modulus obtained for sample 2, 3, 4 and 5.

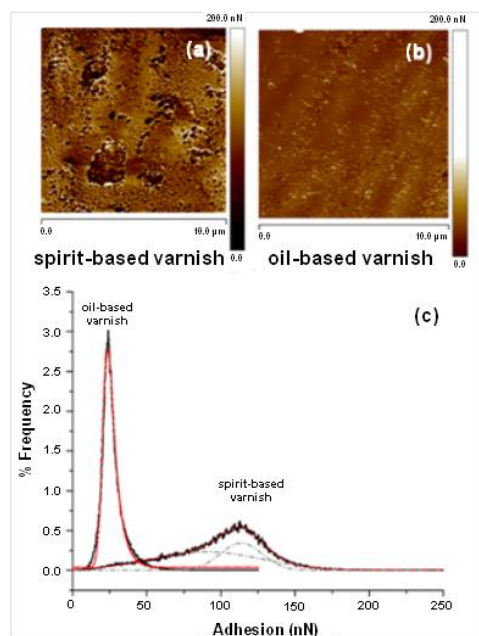


Figure 6. The PeakForce adhesion image of the naturally aged spirit-based sample (sample 6) is shown in (a) and the image for naturally aged oil-based varnish sample is shown in (b). Bearing analysis gave large differences in the distribution of adhesion values for the two samples (c): the oil-based varnish has a narrow range of adhesion values while the spirit-based has a broad distribution and can be fitted to 2 curves, indicating the possibility of greater heterogeneity in the mechanical properties of the surface of the spirit-based varnish.



### 3. Conclusions

In this study it has been demonstrated for the first time that it is possible to obtain AFM images in situ on the surface of a violin using the portable EasyScan 2 AFM instrument. This opens possibilities for imaging on historical violins in collections and for assessment at the nanoscale of the state of preservation of the varnish. Peak force tapping AFM with quantitative nanomechanical analysis provides a tool for assessment of nanomechanical properties of multiphase materials. AFM has provided information on the nano-mechanics of oil-based and spirit-based varnishes and the changes that occur on accelerated ageing. Peak Force AFM has provided additional information on adhesion values. Synchrotron radiation micro-FTIR spectroscopy (SR-FTIR) has provided information on differences in the chemical composition of the varnish layers over the wood and in the depth of penetration of the two varnishes. Examination of the layer structure reveals that the stiffer spirit-based varnish showed less penetration into the wood than the oil-based varnish. This is in accord with observations made by X-ray tomography [1,38]. Information on the extent of penetration into the wood and the change in physico-chemical and mechanical properties with ageing is essential as these properties will contribute to the vibro-acoustical properties of the coated wood as indicated in other papers [1,39,40]. The AFM and nanomechanical studies open up a whole new area of investigation of varnished musical instruments and will provide essential data. Though it has been recognised that the impact of varnish can affect the final sound quality of violins via changes in mechanical properties, there are fewer measurements of, for example, changes in stiffness of varnishes from historical instruments and fewer studies made than of the chemical composition of varnishes from historical instruments [41]. This is mainly due to the invasive nature of mechanical tests generally used. In our study we have shown the potential of non-invasive imaging and the possibility of future non-invasive mechanical measurements on historical instruments.

### 4. Materials and Methods

#### 4.1. Samples

##### 4.1.1. Violin Instrument

The violin which was made available for this study shown in Figure 1a,b had been played for about 40 years. It was bought in 1946 from Boosey & Hawkes (Boosey & Hawkes Music Publishers Limited, Aldwych House, London, UK), and, thus, is likely to be no more than 70 years old. It has never been re-varnished but has been polished with Hidersine 3V violin wax and varnish cleaner (Barnes & Mullins Ltd., Morda, UK).

##### 4.1.2. Model System Samples

For this project, luthier Gabriele Carletti prepared samples using traditional violin varnish recipes. These model systems, shown in Figure 2 and described in Table 1, consist of oil or spirit-based varnish layers on top of maple wood (6 cm × 1.2 cm × 2 cm) over preparation layers of various compositions: water soluble potassium dichromate (also with sodium bicarbonate), cherry gum, gamboge and saffron and then those that are soluble in ethanol and contain dragon's blood and sandalwood. The varnish layers were (a) oil-based containing stand oil, spirit of turpentine, Venice turpentine, Mastic and Sandarac and (b) spirit-based containing ethyl alcohol, Venice of turpentine, Mastic, Elemi, and Shellac (Table 1). All products were Kremer-pigmente GmbH & Co., Aichstetten, Germany.

**Table 1.** Preparation layer composition of a set of varnished wood samples (1 to 6) prepared by Gabriele Carletti which, at the time of analysis, had been naturally aged for a period of four years.

Model System	Preparation Layer Type	Preparation Layer Composition	Varnish Layer Type
1		K <sub>2</sub> Cr <sub>2</sub> O <sub>7</sub>	oil based
2	water soluble	K <sub>2</sub> Cr <sub>2</sub> O <sub>7</sub> + NaHCO <sub>3</sub>	spirit-based
3		cherry gum	
4		gamboge + saffron	
5	ethyl alcohol soluble	dragon's blood	oil based
6		sandalwood	spirit-based

#### 4.2. Atomic Force Microscopy (AFM)

The portable Nanosurf Easyscan 2 AFM operating in intermittent contact mode was used for in situ imaging of the surface of a violin instrument.

#### 4.3. Nanomechanical Measurements

The nanomechanical measurements were performed on the naturally aged samples (4 years after their preparation), which had been stored in the dark, and on the accelerated aged samples.

##### 4.3.1. Young's Modulus Measurement

A Nanowizard 1 AFM (JPK, Bruker, Ettlingen, Germany) was used to measure the Young's Modulus of the model violin samples using a standard force-distance curve approach. The cantilever used for the measurements had a spring stiffness of  $k = 38$  N/m (RTESPA, Bruker, Camarillo, CA, USA) with a setpoint of 500 nN. Samples were adhered to a glass slide using double-sided tape, with the varnish side exposed. Force-distance curves (300) were obtained across three separate areas of  $50 \mu\text{m}^2$  using a Nanowizard (JPK, Berlin, Germany) in contact mode in the air. All FD curves were processed with the Hertzian Model on the proprietary JPK analysis RampDesigner™ software (Budapest, Hungary).

##### 4.3.2. Adhesion Measurement

A Bruker Dimension Icon with PeakForce QNM was used to perform adhesion measurements on the model violin samples. The probe used for the measurements had a spring stiffness of  $k = 6$  N/m (TAP 150A, BudgetSensors, Izgrev, Sofia, Bulgaria) with a setpoint of 10 nN. QNM adhesion images of  $10 \times 10 \mu\text{m}^2$  were obtained at 5 locations across each of the samples. Using the QNM software (open-source Python package), we measured the maximum adhesion for each pixel in the recorded images and pooled the data to plot the Frequency distribution of adhesion for both the oil-based and spirit-based varnish samples.

#### 4.4. Micro-FTIR Measurements

Synchrotron radiation Micro-Fourier Transform Infra-red Analysis (Micro-FTIR) was carried out at the IRIS beamline (BESSY II) at Helmholtz-Zentrum, Berlin (Germany) on a Thermo Nicolet Continuum™ microscope equipped with a mercury–cadmium–telluride (MCT) detector. The sample was mounted on a diamond cell on a motorized microscope stage and raster scanned through the synchrotron beam with a diameter of  $15 \mu\text{m}$  collecting a grid-like pattern of IR spectra spaced in  $10 \mu\text{m}$  increments. Measurements were performed in transmission mode at a magnification  $\times 32$  using confocal objectives. Infrared spectra were registered between  $4000$  and  $650 \text{ cm}^{-1}$  with a spectral resolution of  $4 \text{ cm}^{-1}$ . An accumulation of 128 scans per point was used. Background spectra were collected under identical conditions with only the BaF<sub>2</sub> window on which the sections were placed. The spectrum and mapping acquisition was performed by using the OMNIC Atµs™ software

(Waltham, MA, USA) [42]. The sample preparation protocol consisted of the microtoming at 10 µm of the samples with an embedding-free approach as described in the literature [43].

#### 4.5. Accelerated Aging

Accelerated aging was performed for two weeks after 10 months' natural aging in a Solarbox 1500e RH (Erichsen Cofomegra Instruments, Milan, Italy) purchased from Erichsen (Hemer, Germany). Ageing conditions were as follows: 20 °C, 50%RH, excitation with Xenon lamp (wavelength 280–400 nm) power 400 W. A soda-lime glass UV filter was used to simulate indoor exposure. Irradiation uniformity was guaranteed by a parabolic reflector chamber with the Xenon lamp in focus.

**Author Contributions:** Conceptualization, M.O., S.H., M.P.C. and L.B.; methodology, M.O., S.H., A.L.-T., A.S. and L.B.; formal analysis, A.S., S.H., A.B., A.L.-T., J.J.L. and F.d.G.; investigation, A.L.-T., J.J.L., F.d.G., S.H., A.S., A.B. and L.B.; data curation, M.O. and L.B. writing—original draft preparation, M.O., A.L.-T. and L.B.; writing—review and editing, all authors; supervision, M.O., M.P.C. and L.B. All authors have read and agreed to the published version of the manuscript.

**Funding:** The work benefitted from the outcomes of previous projects including EC 6th & 7th Framework DGXII “Protection & Conservation of European Cultural Heritage”, PROPAIN and 7th Framework projects MEMORI, NANOFORART FP7 project, and participation in WoodMusICK FPS COST action FP1302. The Authors would also like to thank University College London Impact Award and SEAHA for the student funding support. Part of this research was supported by Associazione Liutaria Italiana ALI and the project PRIN 2010–2011: “Sustainability in cultural heritage: from diagnosis to the development of innovative systems for consolidation, cleaning and protection”.

**Institutional Review Board Statement:** Not applicable.

**Informed Consent Statement:** Not applicable.

**Data Availability Statement:** Not applicable.

**Acknowledgments:** Authors wish to specially thank the lute maker Gabriele Carletti for preparing and providing the model systems of varnishes on maple wood. We also thank HZB (Berlin) for the allocation of synchrotron radiation beam time (proposal 15102267-ST) and Emad F. Aziz, and Ulrich Schade from the Institute for Material Development (Berlin, Germany) for her invaluable help while working at the beamline station. Thanks also to Sheikh Khizar and Vishal Panchal at Bruker Nano Surfaces for assistance with data processing.

**Conflicts of Interest:** The authors declare no conflict of interest.

**Sample Availability:** Samples of the compound are available from the authors.

## References

1. Sedighi Gilani, M.; Pflaum, J.; Hartmann, S.; Kaufmann, R.; Baumgartner, M.; Schwarze, F.W.M.R. Relationship of vibro-mechanical properties and microstructure of wood and varnish interface in string instruments. *Appl. Phys. A* **2016**, *122*, 260. [[CrossRef](#)]
2. Echard, J.-P.; Lavédrine, B. Review on the characterisation of ancient stringed musical instruments varnishes and implementation of an analytical strategy. *J. Cult. Herit.* **2008**, *9*, 420–429. [[CrossRef](#)]
3. Lämmlein, S.L.; Mannes, D.; Van Damme, B.; Schwarze, F.W.M.R.; Burgert, I. The influence of multi-layered varnishes on moisture protection and vibrational properties of violin wood. *Sci. Rep.* **2019**, *9*, 18611. [[CrossRef](#)]
4. Odlyha, M.; lluveras Tenorio, A.; Lucejko, J.J.; di Girolamo, F.; Colombini Maria, P.; Bergsten, C.J.; Lopez-Fontal, E.; Hudziak, S.; Strange, A.; Bozec, L. Correlation of Mechanical Behaviour with Advanced Chemical Analysis of Varnished Wood. In Proceedings of the 4th Annual Conference COST FP1302 WoodMusICK, Preservation of Wooden Musical Instruments Ethics, Practice and Assessment, Brussels, Belgium, 5–7 October 2017; p. 202.
5. Odlyha, M.; Bergsten, C.J.; Scharff, M. Wood Science for Conservation of Cultural Heritage. In Proceedings of the International Conference held by COST Action IE0601, Izmir, Turkey, 20–22 October 2010.
6. McLennan, J.E. On varnish. *J. Aust. Assoc. Musical Instrum. Mak.* **2000**, *19*, 16–27.
7. Albano, M.; Comelli, D.; Fiocco, G.; Mattonai, M.; Lucejko, J.J.; Zoia, L.; Colombini, M.P.; Malagodi, M. Chemical modification of wood induced by the traditional making procedures of bowed string musical instruments: The effect of alkaline treatments. *Herit. Sci.* **2022**, *10*, 76. [[CrossRef](#)]

8. Kasprzok, L.; Fabbri, D.; Rombolà, A.G.; Rovetta, T.; Malagodi, M. Identification of organic materials in historical stringed instruments by off-line analytical pyrolysis solid-phase microextraction with on-fiber silylation and gas chromatography-mass spectrometry. *J. Anal. Appl. Pyrolysis* **2020**, *145*, 104727. [[CrossRef](#)]
9. Rovetta, T.; Invernizzi, C.; Fiocco, G.; Albano, M.; Licchelli, M.; Gulmini, M.; Alf, G.; Fabbri, D.; Rombolà, A.G.; Malagodi, M. The case of Antonio Stradivari 1718 ex-San Lorenzo violin: History, restorations and conservation perspectives. *J. Archaeol. Sci. Rep.* **2019**, *23*, 443–450. [[CrossRef](#)]
10. Fiocco, G.; Rovetta, T.; Gulmini, M.; Piccirillo, A.; Licchelli, M.; Malagodi, M. Spectroscopic Analysis to Characterize Finishing Treatments of Ancient Bowed String Instruments. *Appl. Spectrosc.* **2017**, *71*, 2477–2487. [[CrossRef](#)]
11. Caruso, F.; Chillura Martino, D.F.; Saverwyns, S.; Van Bos, M.; Burgio, L.; Di Stefano, C.; Peschke, G.; Caponetti, E. Micro-analytical identification of the components of varnishes from South Italian historical musical instruments by PLM, ESEM–EDX, microFTIR, GC–MS, and Py–GC–MS. *Microchem. J.* **2014**, *116*, 31–40. [[CrossRef](#)]
12. Bonaduce, I.; Odlyha, M.; Di Girolamo, F.; Lopez-Aparicio, S.; Grøntoft, T.; Colombini, M.P. The role of organic and inorganic indoor pollutants in museum environments in the degradation of dammar varnish. *Analyst* **2013**, *138*, 487–500. [[CrossRef](#)]
13. Bertrand, L.; Robinet, L.; Cohen, S.X.; Sandt, C.; Le Hô, A.-S.; Soulier, B.; Lattuati-Derieux, A.; Echard, J.-P. Identification of the finishing technique of an early eighteenth century musical instrument using FTIR spectromicroscopy. *Anal. Bioanal. Chem.* **2011**, *399*, 3025–3032. [[CrossRef](#)] [[PubMed](#)]
14. Echard, J.P.; Cotte, M.; Dooryhee, E.; Bertrand, L. Insights into the varnishes of historical musical instruments using synchrotron micro-analytical methods. *Appl. Phys. A* **2008**, *92*, 77–81. [[CrossRef](#)]
15. Echard, J.-P.; Bertrand, L.; von Bohlen, A.; Le Hô, A.-S.; Paris, C.; Bellot-Gurlet, L.; Soulier, B.; Lattuati-Derieux, A.; Thao, S.; Robinet, L.; et al. The Nature of the Extraordinary Finish of Stradivari’s Instruments. *Angew. Chem. Int. Ed.* **2010**, *49*, 197–201. [[CrossRef](#)]
16. Invernizzi, C.; Fiocco, G.; Iwanicka, M.; Kowalska, M.; Targowski, P.; Blümich, B.; Rehorn, C.; Gabrielli, V.; Bersani, D.; Licchelli, M.; et al. Non-invasive mobile technology to study the stratigraphy of ancient Cremonese violins: OCT, NMR-MOUSE, XRF and reflection FT-IR spectroscopy. *Microchem. J.* **2020**, *155*, 104754. [[CrossRef](#)]
17. Latour, G.; Echard, J.-P.; Soulier, B.; Emond, I.; Vaiedelich, S.; Elias, M. Structural and optical properties of wood and wood finishes studied using optical coherence tomography: Application to an 18th century Italian violin. *Appl. Opt.* **2009**, *48*, 6485–6491. [[CrossRef](#)] [[PubMed](#)]
18. Young, T.J.; Monclus, M.A.; Burnett, T.L.; Broughton, W.R.; Ogin, S.L.; Smith, P.A. The use of the PeakForce™ quantitative nanomechanical mapping AFM-based method for high-resolution Young’s modulus measurement of polymers. *Meas. Sci. Technol.* **2011**, *22*, 125703. [[CrossRef](#)]
19. Bartoletti, A.; Odlyha, M.; Hudziak, S.; Mühlen Axelsson, K.; Groot, J.; Bozec, L. Visibilia ex invisibilibus: Seeing at the nanoscale for improved preservation of parchment. *Insight—Non-Destr. Test. Cond. Monit.* **2017**, *59*, 265–272. [[CrossRef](#)]
20. Vlad-Cristea, M.; Riedl, B.; Blanchet, P.; Jimenez-Pique, E. Nanocharacterization techniques for investigating the durability of wood coatings. *Eur. Polym. J.* **2012**, *48*, 441–453. [[CrossRef](#)]
21. Mao, J.; Abushammala, H.; Kasal, B. Monitoring the surface aging of wood through its pits using atomic force microscopy with functionalized tips. *Colloids Surf. A Physicochem. Eng. Asp.* **2021**, *609*, 125871. [[CrossRef](#)]
22. Casdorff, K.; Keplinger, T.; Burgert, I. Nano-mechanical characterization of the wood cell wall by AFM studies: Comparison between AC- and QI™ mode. *Plant Methods* **2017**, *13*, 60. [[CrossRef](#)]
23. Normand, A.C.; Charrier, A.M.; Arnould, O.; Lereu, A.L. Influence of force volume indentation parameters and processing method in wood cell walls nanomechanical studies. *Sci. Rep.* **2021**, *11*, 5739. [[CrossRef](#)] [[PubMed](#)]
24. Czibula, C.; Seidlhofer, T.; Ganser, C.; Hirn, U.; Teichert, C. Longitudinal and transverse low frequency viscoelastic characterization of wood pulp fibers at different relative humidity. *Materialia* **2021**, *16*, 101094. [[CrossRef](#)]
25. Korte, E.H.; Staat, H. Infrared reflection studies of historical varnishes. *Fresenius J. Anal. Chem.* **1993**, *347*, 454–457. [[CrossRef](#)]
26. Cornea, I.; Cristache, R.; Sandu, I. Characterization of historical violin varnishes using ATR-FTIR spectroscopy. *Rom. Rep. Phys.* **2016**, *68*, 615–622.
27. Rashid, A.M.F.; Hossain, Z. Morphological and nanomechanical analyses of ground tire rubber-modified asphalts. *Innov. Infrastruct. Solut.* **2016**, *1*, 36. [[CrossRef](#)]
28. Ren, D.; Wang, H.; Yu, Z.; Wang, H.; Yu, Y. Mechanical imaging of bamboo fiber cell walls and their composites by means of peakforce quantitative nanomechanics (PQNM) technique. *Holzforschung* **2015**, *69*, 975–984. [[CrossRef](#)]
29. Yamamoto, T.; Sugiyama, S. Structural Changes in Cuticles on Violin Bow Hair Caused by Wear. *Biosci. Biotechnol. Biochem.* **2010**, *74*, 408–410. [[CrossRef](#)]
30. Casado, S. Studying friction while playing the violin: Exploring the stick–slip phenomenon. *Beilstein J. Nanotechnol.* **2017**, *8*, 159–166. [[CrossRef](#)]
31. Heuberger, M.; Dietler, G.; Schlapbach, L. Mapping the local Young’s modulus by analysis of the elastic deformations occurring in atomic force microscopy. *Nanotechnology* **1995**, *6*, 12–23. [[CrossRef](#)]
32. Trtik, P.; Kaufmann, J.; Volz, U. On the use of peak-force tapping atomic force microscopy for quantification of the local elastic modulus in hardened cement paste. *Cem. Concr. Res.* **2012**, *42*, 215–221. [[CrossRef](#)]
33. Schwanninger, M.; Rodrigues, J.C.; Pereira, H.; Hinterstoisser, B. Effects of short-time vibratory ball milling on the shape of FT-IR spectra of wood and cellulose. *Vib. Spectrosc.* **2004**, *36*, 23–40. [[CrossRef](#)]

34. Pandey, K.K.; Pitman, A.J. FTIR studies of the changes in wood chemistry following decay by brown-rot and white-rot fungi. *Int. Biodeterior. Biodegrad.* **2003**, *52*, 151–160. [[CrossRef](#)]
35. Faix, O. Classification of Lignins from Different Botanical Origins by FT-IR Spectroscopy. *Holzforschung* **1991**, *45*, 21–28. [[CrossRef](#)]
36. Faix, O.; Bremer, J.; Meier, D.; Fortmann, I.; Scheijen, M.A.; Boon, J.J. Characterization of tobacco lignin by analytical pyrolysis and Fourier transform-infrared spectroscopy. *J. Anal. Appl. Pyrolysis* **1992**, *22*, 239–259. [[CrossRef](#)]
37. Meier, E. Available online: <https://www.wood-database.com/hard-maple/> (accessed on 30 August 2022).
38. Sedighi Gilani, M. In Stradivari's Footsteps Varnish Affects the Sound of a Violin. Available online: <https://www.empa.ch/web/s604/varnish-and-violins> (accessed on 11 March 2016).
39. Ghaznavi, M.; Rostamisani, A.; Roohnia, M.; Jahanlatibari, A.; Yaghmaeipour, A. Traditional Varnishes and Acoustical Properties of Wooden Soundboards. *Sci. Int.* **2013**, *1*, 401–407. [[CrossRef](#)]
40. Minato, K.; Akiyama, T.; Yasuda, R.; Yano, H. Dependence of Vibrational Properties of Wood on Varnishing during Its Drying Process in Violin Manufacturing. *Holzforschung* **1995**, *49*, 222–226. [[CrossRef](#)]
41. Lämmlein, S.L.; Mannes, D.; van Damme, B.; Burgert, I.; Schwarze, F.W.M. Influence of varnishing on the vibro-mechanical properties of wood used for violins. *J. Mater. Sci.* **2019**, *54*, 8063–8095. [[CrossRef](#)]
42. Puskar, L.; Schade, U. The IRIS THz/Infrared beamline at BESSY II. *J. Large-Scale Res. Facil.* **2016**, *2*, A95. [[CrossRef](#)]
43. Pouyet, E.; Lluveras-Tenorio, A.; Nevin, A.; Saviello, D.; Sette, F.; Cotte, M. Preparation of thin-sections of painting fragments: Classical and innovative strategies. *Anal. Chim. Acta* **2014**, *822*, 51–59. [[CrossRef](#)]